

Article

# Detecting Individual Tree Attributes and Multispectral Indices Using Unmanned Aerial Vehicles: Applications in a Pine Clonal Orchard

José Luis Gallardo-Salazar  and Marín Pompa-García \* 

Faculty of Forest Sciences, University of Juarez del Estado de Durango, Río Papaloapan and Blvd. Durango, Valle del Sur s/n, Durango 34120, Mexico; 1107805@alumnos.ujed.mx

\* Correspondence: mpgarcia@ujed.mx; Tel.: +52-61-81-301096

Received: 5 November 2020; Accepted: 15 December 2020; Published: 18 December 2020



**Abstract:** Modern forestry poses new challenges that space technologies can solve thanks to the advent of unmanned aerial vehicles (UAVs). This study proposes a methodology to extract tree-level characteristics using UAVs in a spatially distributed area of pine trees on a regular basis. Analysis included different vegetation indices estimated with a high-resolution orthomosaic. Statistically reliable results were found through a three-phase workflow consisting of image acquisition, canopy analysis, and validation with field measurements. Of the 117 trees in the field, 112 (95%) were detected by the algorithm, while height, area, and crown diameter were underestimated by 1.78 m, 7.58 m<sup>2</sup>, and 1.21 m, respectively. Individual tree attributes obtained from the UAV, such as total height (H) and the crown diameter (CD), made it possible to generate good allometric equations to infer the basal diameter (BD) and diameter at breast height (DBH), with R<sup>2</sup> of 0.76 and 0.79, respectively. Multispectral indices were useful as tree vigor parameters, although the normalized-difference vegetation index (NDVI) was highlighted as the best proxy to monitor the phytosanitary condition of the orchard. Spatial variation in individual tree productivity suggests the differential management of ramets. The consistency of the results allows for its application in the field, including the complementation of spectral information that can be generated; the increase in accuracy and efficiency poses a path to modern inventories. However, the limitation for its application in forests of more complex structures is identified; therefore, further research is recommended.

**Keywords:** tree-level characteristics; unmanned aerial vehicles; *Pinus* clonal orchard

## 1. Introduction

The world's forests offer a great diversity of goods and services that have led the scientific community to continuously look for new modern and efficient management schemes [1,2]. In fact, the vulnerability of forest ecosystems to climate change [3] and the anthropogenic pressure to which they are exposed [4,5] makes it necessary to better understand the dynamics of forest growth to strengthen decision making for their sustainability.

Given the ecological complexity of forest landscapes, several studies have been directed to promote innovation in forest inventories. In particular, the accurate and automated estimation of tree attributes has been a research trend in recent years. According to a recent study [6], such technologies represent a more efficient means of obtaining detailed information of individual trees, such as total height, diameter at breast height, basal area, tree count, crown delimitation, and volume estimation. For example, Gollob, et al. [7] documented a methodology for diameter estimation, diameter-at-breast-height (DBH) measurement, and tree detection in forest inventory. Lefsky, et al. [8] conducted an approach for the estimation of forest standing volume, obtaining a 95% confidence

interval for the total volume. Similarly, Puliti, et al. [9] measured tree attributes to estimate volume without the use of field data.

The measurement of height and diameter at breast height are fundamental parameters in forest management. Usually, these conjugated variables are essential for the subsequent estimation of volume, biomass, and carbon stocks, so that their proper measurement has a direct impact on the quantification of inventories and thus on decision making [10]. On the other hand, measurements of tree-crown dimensions are important because the tree crown is where trees interact with their surrounding environment, including via diverse physiological processes such as photosynthesis and respiration; consequently, its accurate quantification is crucial to designing strategies of cultural labors on the individual-tree level [11].

In all these studies, a constant has been the application of spatial technologies (i.e., remote sensing) that make estimates more efficient than traditional methods of in situ data collection. Since forest inventories are a laborious and expensive task, the collection of data by remote sensing becomes important in the innovation of forest monitoring. Therefore, the advent of unmanned aerial vehicles (UAVs) and integration with remote sensing have been a turning point in forest management towards the transition of “precision forestry” [6,12].

Furthermore, when these devices are integrated with multispectral sensors, their predictive ability is potentially increased to aspects not visible to the human eye. An evident example is the generation of vegetation indices (e.g., normalized-difference vegetation index (NDVI), green NDVI (GNDVI), and leaf chlorophyll content (LCI)) [13,14] that can provide information on tree vigor and productivity. The recognition of such ecological parameters allows for the early detection of phytosanitary problems and the determination of the conditions of plant phenology [15].

Thus, UAVs represent an area of opportunity with great potential in Mexico, given its floristic diversity and the importance of forest management [16]. Specifically, homogeneous and even-aged forests form an ideal pilot area to study the relevance of using UAVs as modern tools to support modern forestry. In the north of Mexico, there is an established 15-year-old seed orchard of *Pinus arizonica* [17] as a source for preservation and improvement of tree genetic quality. *P. arizonica*, commonly known as the Arizona pine, is one of the most important timber resources in Mexico [18]. Arizona pine is a widely distributed conifer species in the Sierra Madre Occidental, from Southern Arizona to Southern Durango. This species also provides the highest volume and value to the timber industry in northern Mexico due to its abundance and high wood quality. Environmentally, Arizona pine plays a significant role as a source of food and protection for wildlife [17].

Continuous plant-growth monitoring in this seed orchard is a matter of concern for the scientific community and decision makers. Periodic monitoring has led to research new measurement strategies that would increase its effectiveness [19] without undermining its statistical validity. Monitoring quantitative and qualitative variations in individual productivity has serious implications for orchard management [20]. Moreover, these areas require individual and precise measurements to differentially guide management according to inherent spatial characteristics [21,22] to optimize cultural practices [23]. Usually, monitoring the orchard is manual, expensive, and harshly laborious [17]; however, advantages of temporal and spatial resolution offered by UAVs represent a strategic opportunity to improve our geospatial knowledge of the individual dynamics of trees.

Several studies reported the estimation of production parameters such as biomass [24], the measurement of crown structures [25], applications in irrigation [26], pruning architecture [27] and tree counting [28]. Although all these applications mainly used UAVs in fruit growing, to our knowledge, there is still no procedure for the extraction of tree-level characteristics applied to individual trees in Mexico. Knowing these parameters is essential for optimal management in seed orchards, including the proper selection of pruning techniques, irrigation needs, phytosanitary management regimes, and the calculation of tree-level characteristics. In addition, UAV use enables the production of various advanced data such as videos [29,30], orthomosaics [31–33], and digital terrain and surface models [34,35], which contain the basic inputs for subsequent estimates on the individual-tree level.

Under the hypothesis that UAV use significantly improves tree-level estimates regarding direct field measurements, this study proposes a method to estimate tree counts, total height, diameter, and crown area, including basal-diameter (BD) and diameter-at-breast-height (DBH) inferences on the individual-tree level in a pilot area in the north of Mexico. As a complementary objective, an estimation of spectral indices is shown as a strategy for determining the vigor of the clonal orchard.

## 2. Materials and Methods

### 2.1. Study Area

The study site is in the Sierra Madre Occidental in northern Mexico ( $27^{\circ}8'57''N$ ,  $107^{\circ}6'41''W$ ; 2400 m asl) (Figure 1). This region has a variety of ecosystems where pine and oak forests dominate, which resulted from the complexity of physiographic units and climates, and it is located at the transition between the Holarctic and Neotropical regions [36]. The dominant soils are Regosols and Leptosols with loam textures. The climate of the region is semicold, subhumid, with long fresh summers and monsoon rains that are combined with winter precipitation to reach an annual average of 779 mm, and an annual average temperature between 5 and 12 °C [17,37].

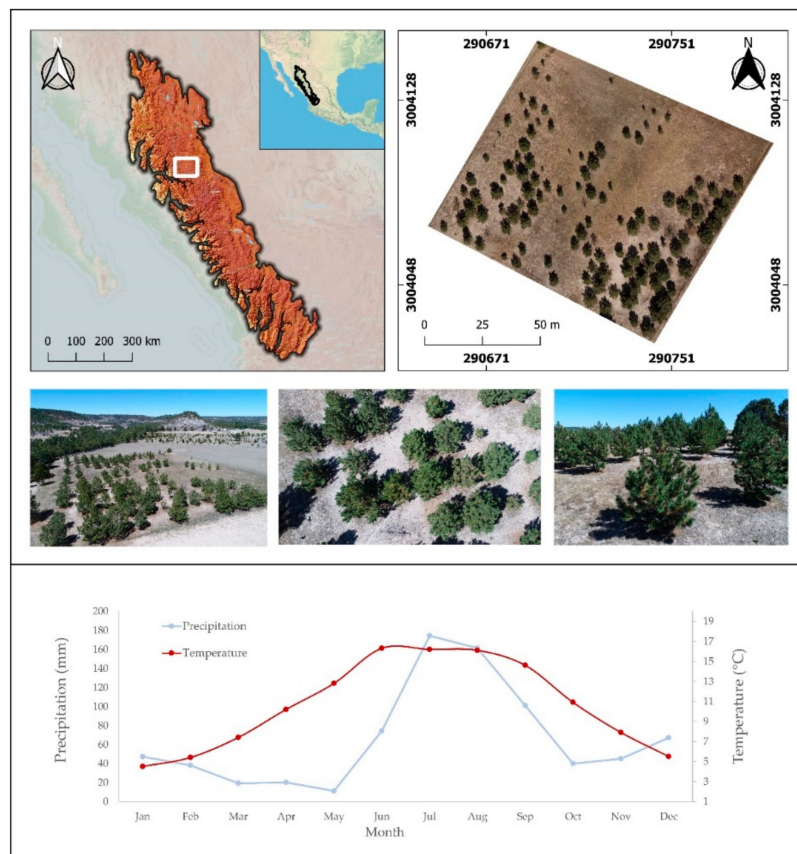


**Figure 1.** View of clonal orchard of *Pinus arizonica* Engelm. and climatogram in the Papajichi ejido, state of Chihuahua, north of Mexico.

This region is one of the most important wood reserves in Mexico, and it is important for commercial timber production and forest conservation [29]. In addition to supplying more than 25% of the timber in Mexico, these forests preserve the main source of springs and streams that feed rivers and reservoirs, which are used for agricultural and public water supplies in the western states of Mexico.

This area is an important and valuable source of ecosystem services (e.g., water, biodiversity, and forest resources) to local populations, and it is a strategically important region for conservation

studies. Particularly since 2005, a portion of 1.10 ha has been considered a clonal orchard area of *Pinus arizonica* Engelm. (Figure 1).

The pine clonal seed orchard was established in 2005 using clones obtained by transplants previously carried out in nurseries. The orchard design is regular, with a real frame arrangement with approximately 6 m spacing between ramets.

## 2.2. Workflow

The general process for the estimates of tree-level characteristics of individual trees using a UAV is illustrated in Figure 2. The first step was flight planning that involved defining the height, and the overlap between images and between lines for the subsequent execution of the flight and image capture.

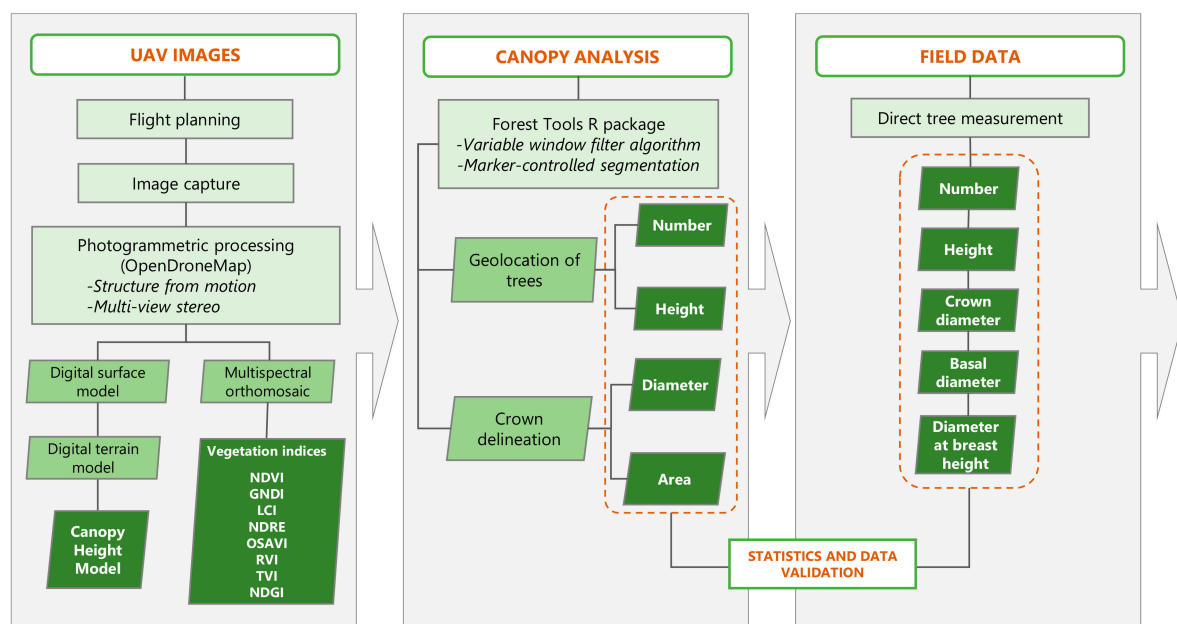


**Figure 2.** Workflow of stages of unmanned aerial vehicle (UAV) image preprocessing, canopy analysis, and validation with field measurements.

Images were processed and analyzed with photogrammetric procedures to derive the digital surface model (DSM) and digital terrain model (DTM) [35]. The canopy height model (CHM) was calculated from the difference in elevation between DSM and DTM. At the same time, multispectral vegetation indices were calculated as a strategy to test the phytosanitary status of the orchard. Canopy analysis involved detecting and geolocating trees in the clonal orchard, estimating heights, and delimiting crowns to obtain diameters and crown areas. Lastly, the estimation of tree-level characteristics calculated with the UAV was evaluated with respect to those recorded in the field by correlation analysis.

## 2.3. UAV Image Acquisition and Processing

On 17 October 2020, the study area was overflowed using a DJI Phantom 4 Multispectral (P4M) quadcopter (Figure 3a). The P4M camera has a total of 6 imaging sensors—5 multispectral sensors (i.e., blue, green, red, red-edge, and near-infrared bands) and 1 RGB sensor, all with a global 2 MP shutter (Table 1). The focal length of the P4M camera is 5.74 mm, image size is 1600 × 1300 pixels, and sensor size is 4.87 × 3.96 mm [38]. The P4M demonstrated good accuracy, yield, and consistent data generation [39].



**Figure 3.** (a) DJI Phantom 4 Multispectral UAV used for image acquisition; (b) first and (c) second grid of flight planning, both made using DJI Ground Station Pro application.

**Table 1.** Spectral-band information for Dà-Jiāng Innovations (DJI) Phantom 4 Multispectral (P4M).

Band	Central Wavelength (nm)	Wavelength Width (nm)
Blue	450	32
Green	560	32
Red	650	32
Red-edge	730	32
Near-infrared	840	52

The flight plan for automatic image acquisition was programmed with the DJI Ground Station Pro application [40]. A  $109 \times 107$  m double grid was established, covering the entire clonal orchard with an overlap of 80% between photos and 70% between lines. Flight height was 60 m above ground level (AGL) with a camera angle of  $90^\circ$  and  $75^\circ$  for the first and second grid, respectively (Figure 3b).

The P4M operates under the principle of direct onboard georeferencing. In other words, it is equipped with a global positioning system (GPS) that geotags the coordinates of each acquired image. This indicates that the acquired images were directly georeferenced by the GPS capability during the flight mission [41]. It was not necessary to use the real-time-kinematic (RTK) system because the P4M manufacturer reported that the georeferencing system can reach vertical and horizontal location pressure of  $\pm 0.1$  and  $\pm 0.3$  m, respectively [42].

From the captured RGB and multispectral images, photogrammetric and computer-vision procedures were applied using free and open-source software OpenDroneMap (ODM) [43]. Outputs from ODM and the commercial options are similar; however, a major advantage is cost and its inherent feature of being an open-source software offers multiple options to customize photogrammetric procedures, decrease processing time, and increase documentation available to users. [44].

This software implements the modern Structure from Motion (SfM) and Multi-View Stereo (MVS) algorithms, showing common characteristics in images with a high percentage of overlap. It then generates a 3D point cloud of 1000–20,000 points  $\text{m}^{-2}$  [9] from which it filters and interpolates a DSM and DTM, which, in turn, are used to orthorectify each image and construct an orthomosaic [45,46]. This process generated the RGB orthomosaic, multispectral orthomosaic, DSM, and DTM of the clonal orchard. The raster calculator was used with free and open-source QGIS software [47], and the following equation was applied [48] to generate a canopy-height model (CHM) to represent the potential height of each tree:

$$\text{CHM} = \text{DSM} - \text{DTM} \quad (1)$$

where CHM is the canopy-height model, DSM is the digital surface model, and DTM is the digital terrain model.

#### 2.4. Estimates of Tree-Level Attributes

There are many methods for the detection and delimitation of individual tree crowns in different forest scenarios [49,50]. The ForestTools package [51] from statistical software R [52] was used in this study. This package was designed to work with CHM LiDAR data or photogrammetric point cloud derived from UAV photogrammetry. In short, the package automatically detects tree crowns, obtains tree height (m), generates polygons, and calculates the crown area ( $\text{m}^2$ ). From there, the following formula was used to find the crown diameter (m) of each tree present in the clonal orchard:

$$d = 2 \sqrt{\frac{a}{\pi}}, \quad (2)$$

where  $d$  is the crown diameter and  $a$  is the crown area.

Initially, a Gaussian filter was applied to smooth the CHM to remove heterogeneity in pixel values [53]. The size of the filter was determined by setting the standard deviation parameter (0.75), which is in units of grid cells using free and open-source WhiteboxTools software [54]. Subsequently, the ForestTools package was implemented as a tool to individually geolocate trees and delimit tree crowns through the variable-window-filter (vwf) algorithm [55] and the marker-controlled segmentation algorithm proposed by Beucher and Meyer [56], respectively.

Field data were collected on the same day of the flight (17 October 2020) and correspond to the beginning of the species' dormancy stage [17]. Each individual tree in the clonal orchard was detected, manually tagged, and rigorously measured. Basal diameter (BD; cm) and diameter at breast height (DBH; cm) were recorded using a diameter tape. Tree heights (m) were recorded using a level staff. Average crown diameter (m) was also obtained by recording the width of the horizontal crown projections (east–west and north–south) for each tree using a measuring tape. Crown area ( $\text{m}^2$ ) was obtained from the average crown diameter, and the following formula was applied:

$$a = \pi \frac{d^2}{4}, \quad (3)$$

where  $a$  is the crown area and  $d$  is the average crown diameter.

However, crown-area calculation assumes a circular geometric pattern, which in the field is usually irregular in shape and spatial extension. For this reason, delimitation of this attribute by means of a UAV recovers relevance, since it is considered to be a better approximation to the precise spatial conformation of the individual.

To compare the estimates of tree-level characteristics obtained with the UAV with respect to field measurements, we used correlation analysis to estimate the degree of correspondence between estimated variables and those recorded with field data. Moreover, simple regression models were used to estimate adjustment efficiency regarding the determination coefficient ( $R^2$ ) and root-mean-square-error (RMSE) by means of statistical software R [52]. Furthermore, the fulfillment of regression assumptions [57] used in forest modeling was verified. Attributes were classified to increase the goodness of fit and explore the potential improvements of statistical parameters [58].

Given the goodness of estimation of certain variables from the UAV, using allometric relations equations were obtained to predict the BD and the DBH. From a practical point of view, this strategy allows for enhancing the use of individual tree-level attribute measurements, saving time and improving certainty.

### 2.5. Multispectral Image Analysis

Since vegetation indices are proxies of vegetation vigor or productive status [13,14], we also tested multispectral vegetation indices recorded from the UAV in the study area. These indices were estimated from the multispectral orthomosaic with the QGIS raster calculator (Equations (4)–(11)):

$$\text{NDVI} = \frac{\text{NIR} - \text{RED}}{\text{NIR} + \text{RED}} \quad (4)$$

$$\text{GNDVI} = \frac{\text{NIR} - \text{GREEN}}{\text{NIR} + \text{GREEN}} \quad (5)$$

$$\text{LCI} = \frac{\text{NIR} - \text{RedEdge}}{\text{NIR} + \text{RED}} \quad (6)$$

$$\text{NDRE} = \frac{\text{NIR} - \text{RedEdge}}{\text{NIR} + \text{RedEdge}} \quad (7)$$

$$\text{OSAVI} = \frac{\text{NIR} - \text{RED}}{\text{NIR} + \text{RED} + 0.16} \quad (8)$$

$$\text{RVI} = \frac{\text{NIR}}{\text{RED}} \quad (9)$$

$$\text{TVI} = \sqrt{\frac{\text{NIR} - \text{R}}{\text{NIR} + \text{R}} + 0.05} \quad (10)$$

$$\text{NDGI} = \frac{\text{GREEN} - \text{RED}}{\text{GREEN} + \text{RED}} \quad (11)$$

where NDVI, the normalized difference vegetation index that is the most used indicator of the chlorophyll content in vegetation, provided information about vegetation growth and nutrients. GNDVI, green NDVI, uses a green band, which represents the surface, instead of the red used in NDVI. GNDVI can show whether vegetation is lacking water or nutrients or is suffering from postmaturity biomass recession. LCI, leaf chlorophyll content, is an important index for evaluating vegetation growth and yield. It is also an indicator for evaluating plant nutrient stress, disease, growth, and aging. NDRE, normalized difference red-edge index, uses a red-edge band instead of the red used in NDVI. This red-edge band is a spectral region in the transition zone from the red spectrum to the near-infrared spectrum. NDRE can be used for managing vegetation based on variables such as chlorophyll and sugar content. OSAVI, soil-adjusted vegetation index, is based on NDVI and relevant observation

data. This index is used for removing the impact of soil conditions on vegetation. RVI, ratio vegetation index, indicates the presence of vegetation and correlates with the amount of vegetation in particular fields. Its values can increase far beyond 1; very high values are generally on the order of 30. TVI, transformed vegetation index, modifies NDVI by adding a constant of 0.5 to all its values and taking the square root of the results. The 0.5 constant is introduced in order to avoid operating with negative NDVI values. Moreover, there is no technical difference between NDVI and TVI in terms of image output or active vegetation detection. NDGI, normalized difference greenness index, is based on reflectance values in the visible spectrum of radiation. This index can provide information about differences in the content of various pigments and variation throughout the entire vegetation season [59].

### 3. Results

A total of 2340 images were captured. Of these, 390 images were from the RGB sensor. Figure 4 shows the RGB orthomosaic, DMT, DSM, and CHM derived from the photogrammetric process with ODM. The coverage area of these products is 1.10 ha and has a spatial resolution [60] or ground sampling distance (GSD) of 4 cm.

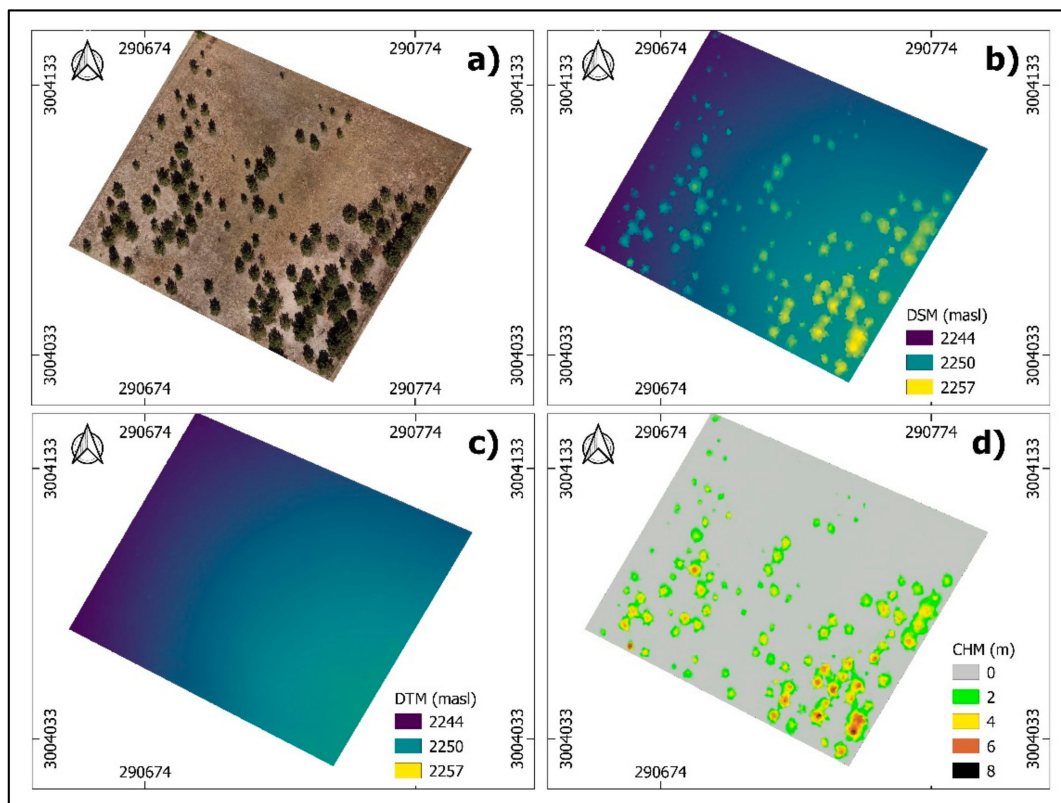


**Figure 4.** (a) RGB orthomosaic, (b) digital surface model, (c) digital terrain model, and (d) canopy-height model derived from UAV flight.

In the field study, 117 trees in the clonal orchard were recorded and measured. Table 2 shows the descriptive statistics of tree-level characteristics recorded in the field. Using the variable-window-filter algorithm of the ForestTools package, 95% of the trees (i.e., 112 out of 117) were detected, and their tree crowns were delimited. Although the trees are the same age, the phenotypic conformation is variable [17], and their open and regular canopy (Figure 5) was strategic for the purposes of the study.

**Table 2.** Descriptive statistics of 117 trees from *Pinus arizonica* Engelm. clonal orchard.

Descriptive Measurement	BD (cm)	DBH (cm)	H (m)	CD (m)	CA (m <sup>2</sup> )
Minimum	7.64	2.22	1.15	0.76	0.45
First quarter	16.55	13.21	4.60	3.37	8.94
Average	21.22	16.25	5.63	4.72	19.26
Median	20.69	15.59	5.70	4.63	17.53
Third quarter	26.10	19.99	6.70	6.00	28.27
Maximum	36.76	38.19	10.20	8.65	58.76

Note: BD, basal diameter; DBH, diameter at breast height; H, height; CD, crown diameter; CA, crown area.

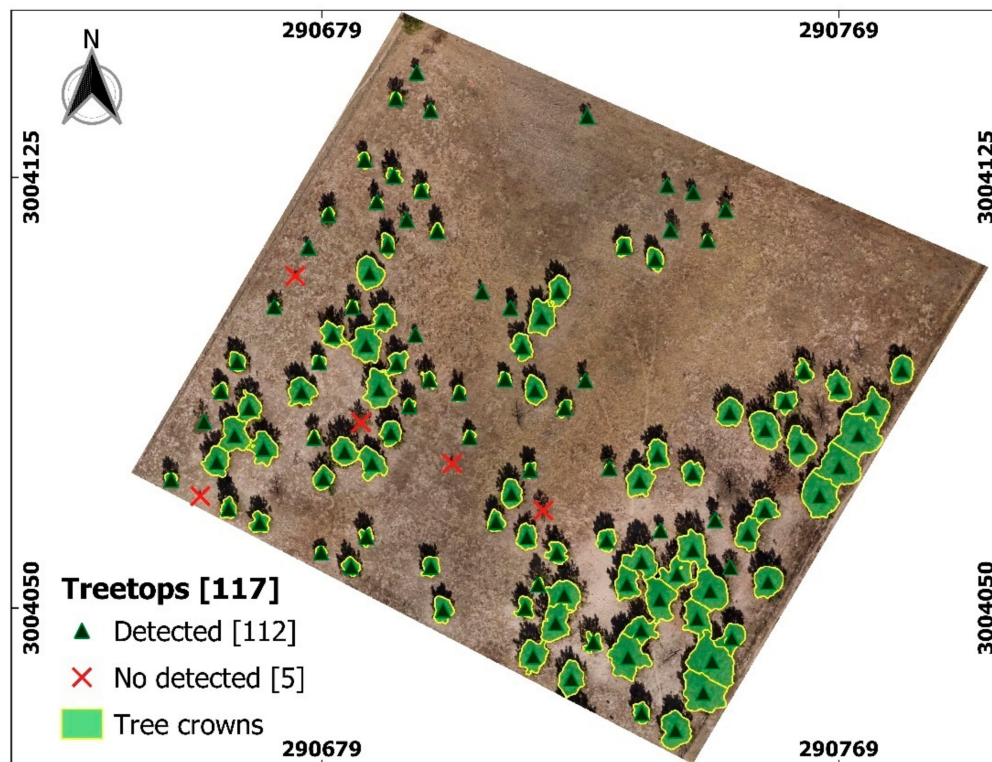


**Figure 5.** Detection and delimitation of individual tree crowns from canopy-height model (CHM) with the ForestTools package.

Statistical evaluations of tree-level characteristics recorded with field data and those estimated with UAV are summarized in Table 3. Height, area, and crown diameter were underestimated by the UAV by 1.78 m, 7.58 m<sup>2</sup>, and 1.21 m, respectively. High and positive correlation was observed between height, area, and crown diameter recorded with field data and those estimated with the UAV. That is, the values of correlation coefficients ( $r$ ) are close to 1.0 (0.97, 0.95, and 0.95, respectively). In general, RMSE and bias values indicated high consistency between measurements of tree-level characteristics. Although class rankings were made as suggested by Wang, Lehtomäki, Liang, Pyörälä, Kukko, Jaakkola, Liu, Feng, Chen, and Hyyppä [58], no better estimates were found than those obtained in total, as presented below.

**Table 3.** Statistical evaluations of tree-level characteristics recorded and estimated from 112 trees detected in the clonal orchard.

	Height (m)		Crown Area (m <sup>2</sup> )		Crown Diameter (m)	
	c	e	c	e	c	e
Minimum	2.05	1.05	1.59	0.06	1.42	0.27
First quarter	4.79	3.12	9.59	3.80	3.49	2.20
Average	5.76	3.98	19.93	12.35	4.75	3.54
Median	5.77	3.93	18.28	10.16	4.82	3.59
Third quarter	6.78	4.76	28.57	18.81	6.03	4.89
Maximum	10.20	7.25	58.76	46.60	8.65	7.70
RMSE	0.36		3.88		0.47	
Bias	$-5.46 \times 10^{-5}$		$2.17 \times 10^{-4}$		$-3.57 \times 10^{-5}$	
$r$ ( $p < 0.001$ )	0.97		0.95		0.95	

c, recorded with field data; e, estimate using UAV; RMSE, root-mean-square error.

Figure 6 shows the results of linear regression applied in order to determine the relationship between data recorded with field data and those estimated with UAV; a graph of residues against predicted values (i.e., height, area, and crown diameter) is also included. For height recorded in the field, corresponding to the 112 trees detected, the model was able to explain 95% of variability observed from that tree-level characteristic ( $R^2 = 0.95$ ) with an RMSE of 0.36 m (Figure 7). Similarly, the linear model for the crown-area variable had a determination coefficient of 90% ( $R^2 = 0.90$ ) and an RMSE of 3.88 m<sup>2</sup> (Figures 6b and 7). Lastly, the model for the crown diameter was able to explain variability observed in 91% of that tree-level characteristic ( $R^2 = 0.91$ ) with an RMSE of 0.47 m (Figures 6c and 7).

For the inference of BD and DBH, all attributes calculated with the UAV (i.e., height, crown area, and crown diameter) were tested. The best-fitting predictor variables were determined by the following equations:

$$\text{DBH} = 0.4966 + 4.1123 H, \quad (12)$$

where DBH is the diameter at breast height and H is the height estimate using a UAV.

$$\text{BD} = 10.3006 + 3.2024 \text{CD}, \quad (13)$$

where BD is the basal diameter and CD is the crown-diameter estimate using a UAV.

The DBH and BD models showed favorable goodness of fit. The estimated height with UAV was the predictor variable that better explained DBH variability ( $R^2 = 79\%$ ,  $p$  value  $2.2 \times 10^{-16}$ ) and an RMSE of 2.81 cm, while BD was better inferred by CD, explaining the variability of this parameter in 76% ( $R^2$ ) with an RMSE of 2.73 cm. The  $p$  value of both models was significant ( $2.2 \times 10^{-16}$ ), which confirmed a statistical relationship (not random). The statistical significance of the coefficients of the independent variables is shown in Table 4.

**Table 4.** Simple regression coefficients predicting basal diameter and diameter at breast height.

Dependent Variable	Independent Variables	B	Standard Error	t	Significance
Diameter at breast height	Constant	0.4966	0.8031	0.603	0.548
	Height estimate using UAV	4.1123	0.1979	20.781	$<2 \times 10^{-16}$
Basal diameter	Constant	10.3006	0.5825	17.68	$<2 \times 10^{-16}$
	Crown-diameter estimate using UAV	3.2024	0.1469	21.80	$<2 \times 10^{-16}$

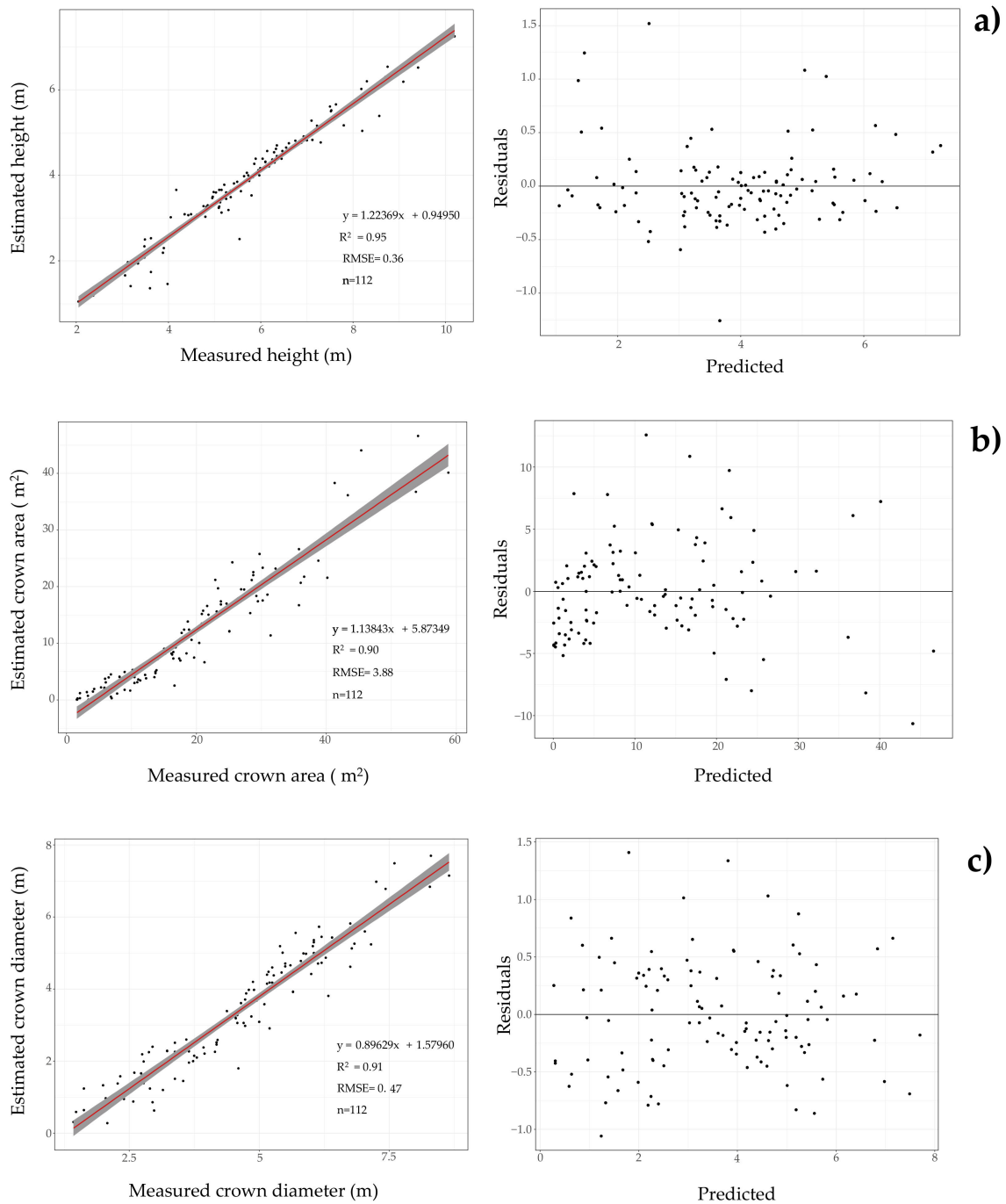


**Figure 6.** Regression analysis and graph of residues against predicted values for tree-level characteristics with field data vs. those estimated with UAV from 112 trees detected. (a) Height; (b) crown area; (c) crown diameter.

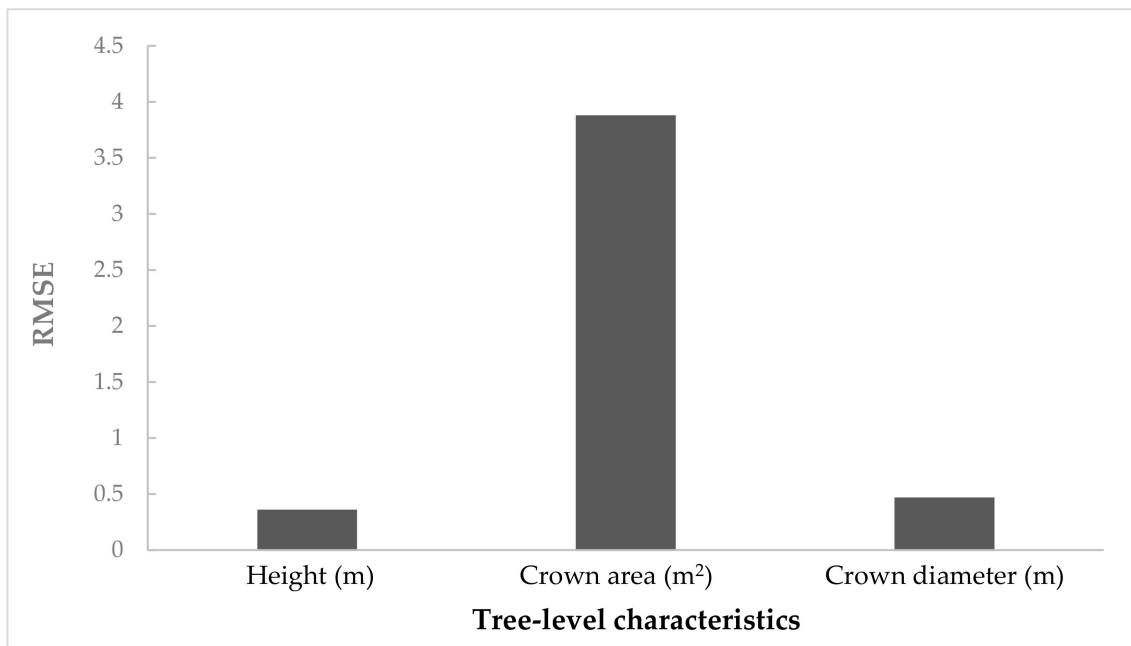


**Figure 7.** Absolute RMSE of simple regression models for tree-level characteristics with field data vs. those estimated with UAV.

Figures 8 and 9 show the scatter diagrams between each predictor and residues for each model. Therefore, it was possible to check the condition of the linear relationship between numerical predictors and response variable (i.e., if the relationship were linear, residuals would be randomly distributed around 0 with constant variability along the X axis).

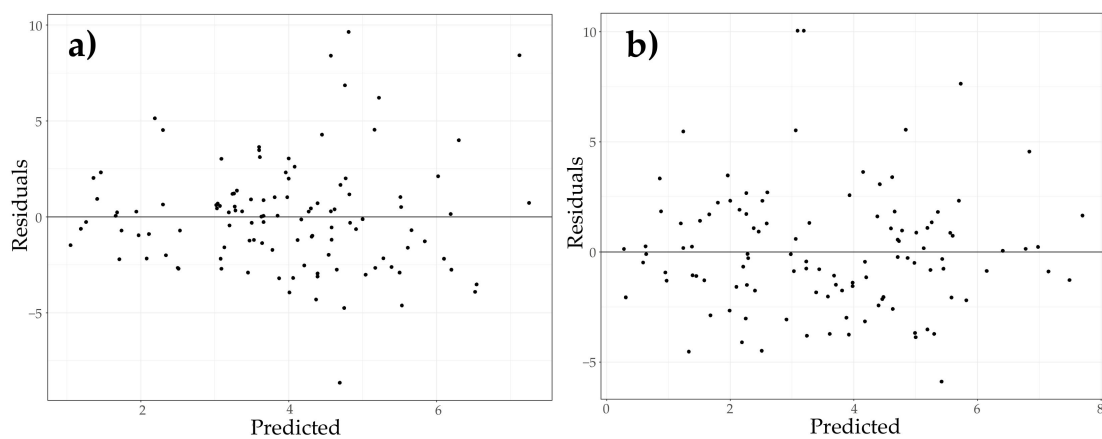


**Figure 8.** Graph of residues against predicted model values. (a) Diameter at breast height and total height estimated with UAV; (b) basal diameter and crown diameter estimated with UAV.

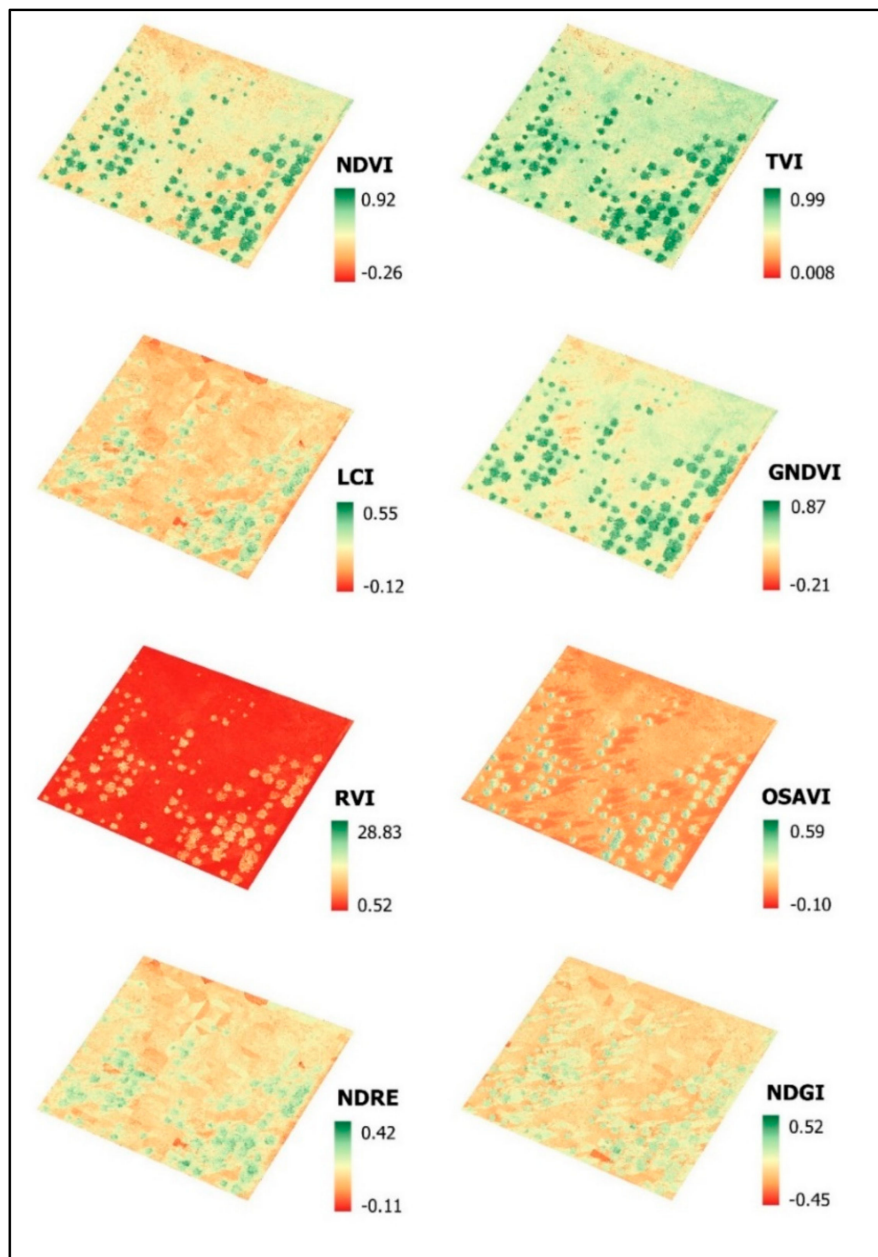


**Figure 9.** Vegetation indices in *Pinus arizonica* Engelm. clonal orchard.

Regarding vegetation-index estimates, 1950 images were captured with P4M's multispectral sensors (i.e., blue, green, red, red-edge, and near-infrared bands). Figure 9 shows the different vegetation indices calculated for the clonal orchard from the multispectral orthomosaic derived from photogrammetric processing with ODM. Moreover, Figure 10 shows the distribution of the average values of vegetation indices corresponding to tree crowns. The estimated indices were NDVI, TVI, LCI, GNDVI, RVI, OSAVI, NDRE, and NDGI; Table 5 shows the descriptive statistics of the values of these indices.

**Table 5.** Descriptive statistics of vegetation indices in *Pinus arizonica* Engelm. clonal orchard.

Descriptive Measurement	NDVI	TVI	LCI	GNDVI	RVI	OSAVI	NDRE	NDGI
Average	0.36	0.63	0.16	0.39	2.74	0.10	0.13	−0.02
Maximum	0.92	0.99	0.55	0.87	28.85	0.59	0.42	0.52
Minimum	−0.26	0.008	−0.12	−0.21	0.52	−0.10	−0.11	−0.45
Standard deviation	0.18	0.14	0.08	0.14	2.32	0.09	0.06	0.11

NDVI, normalized difference vegetation index; TVI, transformed vegetation index; LCI, leaf chlorophyll index; GNDVI, green NDVI; RVI, ratio vegetation index; OSAVI, optimized soil adjusted vegetation index; NDRE, normalized difference red edge index; NDGI, normalized difference greenness index.

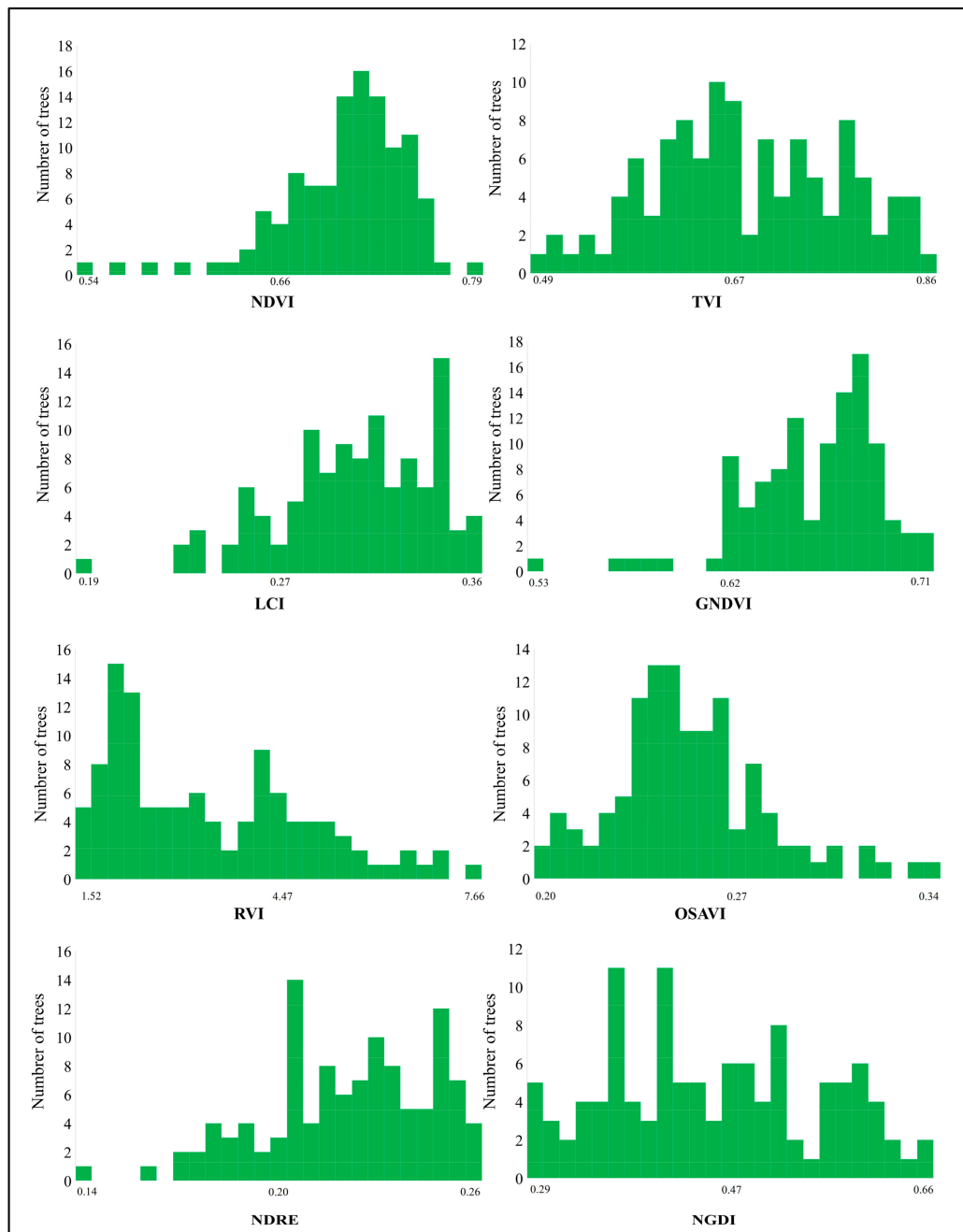


**Figure 10.** Individual-tree vegetation-index distribution in *Pinus arizonica* Engelm. clonal orchard.

Tree-crown vegetation-index values were visually recognizable on the higher levels (i.e., green and yellow shades; Figure 9). Difference was evident between tree crowns and surfaces different from tree crowns (i.e., orange and red shades), corresponding to bare soil or provided with herbaceous vegetation. However, for all indices, high and low values could be recognized within the tree crowns, attributable to different levels of health or stress. Consequently, each index had a different histogram shape (Figure 10). According to Minařík and Langhammer (2016), the divergent shape of histograms implies the different sensitivity of the indices to separate categories of forest disturbance and/or productivity, highlighting NDVI as the one with the best capacity.

Regarding the distribution of the average values of the vegetation indices, NDVI showed an average of 0.70, with 86% of the trees having values between 0.66 and 0.78. From qualitative analysis, trees with high NDVI values coincided with those of GNDVI; however, the average value of this index was 0.65 for most of the trees (91%), with values from 0.62 to 0.71. NDRE had an average value of 0.2, which could be attributed to the fact that this index is a good indicator when large quantities of chlorophyll have already accumulated. On the other hand, LCI determines chlorophyll content, so it is in a lower range than that of the above-mentioned indices; the maximal value for this index was 0.36 and the minimal was 0.19, with an average of 0.30. For OSAVI, tree crowns had average values between 0.20 and 0.34, and 59% of the trees were in a range of values of 0.23 and 0.27. TVI removes negative NDVI values; the average of this index was 0.68, ranging from 0.49 to 0.86. This highlighted the higher values at the tree crowns and allowed for them to be differentiated from the rest of the coverage in the orchard. RVI is characterized by discriminating the presence of vegetation with high greenness with respect to other types of cover. The average value for this index was 3.5 with a minimum of 1.5 and a maximum of 7.7. NDGI values fluctuated from 0.29 to 0.65. This index is highly sensitive to minimal changes in vegetation under subsequent fire or drought conditions. Figure 10 shows that this index is less contrasting to define tree crowns and highlights the photosynthetic activity in the surrounding areas with the presence of herbaceous vegetation.

#### 4. Discussion

To our knowledge, this is the first approach to estimate tree-level attributes and multispectral indices using UAV in a pine clonal orchard; although it is an area with trees regularly distributed in space and of similar age, findings may lead to improving the context of current inventories.

In fact, the recent literature reported exponential interest of UAV applications in the estimation of structural attributes during the last five years [6], and contributes to improving those technologies with limitations in temporality and spatial resolution that complicate more realistic mapping in small areas [61]. Thus, our findings in terms of the calculation of height, crown attributes, and tree counts estimated using UAV offer a promising future in forest-resource management towards precision forestry [2,6,62].

Height estimation is a typical parameter in forest management since it is a basic input for calculating volume, and it is usually a parameter of forest productivity, including carbon stocks [63]. Although the study orchard was directly and rigorously telescoped (some cases involving tree climbing), accuracy and precision were limited to higher heights [58]. Optionally, our remote-sensing methodology offered a solid estimate (Table 3); however, it underestimated by 1.78 m, which could be attributed to the limited generation in the cloud of points at the tree apex. According to Krause, Sanders, Mund, and Greve [63], the photogrammetric dataset implicitly had this error, and it is considered acceptable and often attributed to the leaning angle. Furthermore, according to the standardization of typical forest inventories, an error of 10% is allowed, which is valid for practical purposes [64].

Height measurements by a technician in the field are usually performed with indirect methods where clear visibility is required from the base to the top of the tree; despite the technician's attempts to control this error, under natural conditions visibility can be restricted due to the complexity of the shape of the crown, the occlusion of neighboring trees, very steep slopes, etc. Therefore, the implication of errors in the field could be greater than that obtained by the UAV (Figure 7), so our approach is viable in

operational terms. However, to significantly improve accuracy, Krause, Sanders, Mund, and Greve [63] recommended repeating the missions with the consequent gain in data quality and quantity, especially in new and fast-growing species. Likewise, georeferencing individuals to an acceptable level of precision gives them a strategic advantage over expensive and time-consuming fieldwork.

Comparatively, the results of height estimation can be considered acceptable in their estimates with those of Wu, et al. [65] ( $R^2 = 0.89$ , RMSE = 0.19 m, rRMSE = 5.37%); Roşca, et al. [66] (RMSE 0.11–0.63 m); Krause, Sanders, Mund and Greve [63] (RMSE values of 0.304 m (1.82%) and 0.34 m (2.07%), respectively ( $n = 34$ )); and Falkowski, et al. [67] measurements of tree height ( $r = 0.97$ ) and crown diameter ( $r = 0.86$ ), albeit in different species and under different environmental conditions, so further research should be conducted as suggested on variations in slopes, densities, complexity, and crown classes [58]. Although the same author reported that the results were improved by the classification of attributes, our study found no benefit when classifying them (R and RMES values were lower).

With respect to contour and crown-area measurements, these estimates are more important as tree-level characteristics that can be used to estimate other attributes such as volume, biomass, and carbon. Wu, Johansen, Phinn, Robson and Tu [65] highlighted the importance of this characteristic to design better cultural practices on the individual-tree level, detect physiological activity, and for phenological monitoring (production, cone quality, pruning). Above all, its metric input is potentially strategic for precision forestry [2,12]. Assessing the absolute accuracy of UAV-based results requires independent and alternative measures. However, for the measurements of diameter and crown area, it was not possible to have real data because of irregular geometrical tree characteristics. Real field measurements are laborious and inaccurate because they assume a circular geometric model, unlike the more accurate results offered by the aerial perspective where tree crowns are favorably visualized according to their exact shape and spatial extension.

Therefore, to achieve a more accurate estimation of crown area and crown diameter, it is advisable to take multiple measurements with the UAV until standard deviations are minimized to the desired level. Other mission parameters must be considered to find the optimal one (e.g., flight heights) [68]. Compared to the study by Johansen, Raharjo and McCabe [68], the GEOBIA algorithm and eCognition Developer 9.2 software found an  $R^2 = 0.96$  and RMSE of 0.6 m, although they tested different heights, and the crown area was not measured in the field. In addition, in such a study, mapping was improved in the youngest (smallest) trees, which showed differential estimates according to tree dimensions; however, as mentioned in this study, such classification did not yield statistical improvements.

Despite the promising results (Table 3 and Figure 6), crown delineation is complicated in trees that occlude neighboring trees with their branches, so caution is required in applying this approach with those dense stands [58]. It is also recommended to complement with other technologies such as those of 2D spatial-wavelet analysis by Falkowski, Smith, Hudak, Gessler, Vierling, and Crookston [67].

Although analysis incorporating two or more species is beyond the objectives of this research, we expect that high tree densities would make it difficult to model, at least with these sensors, since tree-crown measurements in old growth stands are labor-intensive and imprecise because of the difficulty of observing them from the ground. In this case, sensors such as terrestrial laser scanning that can cross the canopy are recommended. According to Ritter and Nothdurft [69], these technologies have proven their efficiency in other geographical areas.

In relation to tree count, the potential usefulness of the developed algorithm is evident; the high rate of found precision (112/117), despite phenotypical differences in individuals, reflects the relevance of the followed approach. This coincides with recent findings generated in other latitudes, such as the case of Jiménez-Brenes, López-Granados, de Castro, Torres-Sánchez, Serrano, and Peña [27], which reported 80% of the trees in an olive orchard. It is recommended to research in more detail the configuration of different parameters of the flight [68], which could yield better tree-counting efficiency. On the other hand, the large amount of travel time required for individual field counts is drastically reduced by the procedure followed here. This gives a high degree of practical application to

the results towards aerial inventories [9], which, combined with allometric equations, could calibrate forest-growth models, forest management, and studies of forest ecology.

Thus, our workflow is solid and important, particularly for monitoring small sites on a continuous and permanent basis, including the complementation of spectral information that could be generated. For example, tree-level attributed results were obtained only by RGB imaging (Figure 4a), while multispectral sensors (i.e., blue, green, red, red-edge, and near-infrared bands) augmented the data quality of the results. Taken together, the derived products are revolutionizing forest monitoring.

The use of UAVs has been increasing, and multiple innovation choices are projected for forest monitoring and assessing tree attributes [6,58]. The capacity for capturing high-resolution imagery, even in the presence of clouds, comparatively enhances the quality of data with respect to traditional Earth-observing satellites. Hence, research perspectives are expanded to tree-level attribute detection and forest-health monitoring. Particularly, the emergence of modern sensors and linked platforms are stand-out opportunities to improve the knowledge of forest dynamics.

By combining remotely sensed data products from UAV with other related disciplines, it is possible to more accurately detect tree-level characteristics, including tree physiological stress, due to the high sensibility of multispectral sensors. Furthermore, the cost of UAVs and their associated platforms is rapidly decreasing, while the number of sophistication and flexibilization procedures is increasing [6]. Opportunities offered by processing methods indicate significant progress to augment analysis framework capabilities. For instance, free and open-source software platforms are becoming popular and provide alternatives for the estimation of tree-level attributes, such as above-ground biomass and stem volume [44].

However, there is still the need to improve the distortion of camera calibration. Some authors suggested to increase the checkpoints using on-board differential GPS systems, such as real-time-kinematic (RTK) or postprocessing-kinematic (PPK) technologies, although in practical applications, they are costly, and most forestry applications on this geographic scale are enough, as shown here [19]. Results also cannot be extrapolated to forests with more complex structures, such as unevenly aged stands. They are different from those studied here, where uniformity and spatial arrangement allowed for the easy distinction of individuals. Therefore, the next challenge is to continue with further research in natural forests that are representative of forest ecosystems that are under some kind of management, including areas of conservation and protection.

The application of vegetation indices represents a significant contribution towards precision forestry. For example, spatial distribution in Figure 9 describes local variations in vigor that an orchard manager cannot detect on the field. This spatial variation in individual productivity suggests a tool for growers in terms of differential individual-tree management. Similar results were documented by Grulke, et al. [70].

The values of vegetation indices showed a different histogram shape (Figure 10). According to Zhao, et al. [71], the divergent form of histograms reflects the different sensitivity of indices in terms of separating categories of forest disturbance and/or productivity, highlighting NDVI as the index with the greatest capacity. This is in line with the results of Brovkina, et al. [72], who considered NDVI to be a good vigor indicator.

GNDVI values were higher than those reported by Wahab, et al. [73], which may indicate greater photosynthetic activity, so it is recommended as a parameter for monitoring variations in leaf chlorophyll and vegetation health [74]. In addition, the OSAVI threshold for tree crowns in the clonal orchard suggested that green aerial biomass stored was greater than that of the subsoil [75]. According to Minařík and Langhammer [76], NDRE results suggested that *P. arizonica* crowns are consistent with mostly healthy trees in *Picea abies* forests. However, our RVI results were lower than those reported by Xing, et al. [77], which is probably attributed to differences in the used sensors since, to our knowledge, this is the first study that generated such values from a UAV; consequently, comparisons with others studies lack contrasting parameters.

We recognize the limitations of vegetation-index approaches, such as phytosanitary parameters. For example, although NDVI was the best vigor proxy, it is necessary to improve its discrimination values; grass or weed residues can decrease the predictive capacity of NDVI, and crown size and superposition can reduce the use of remote sensing on the tree level [78,79]. In this case, soil-management practices such as drainage, tillage, and traffic control are recommended, with implicit benefits for tree development. Another difficulty is related to the problem of estimating the differentiated temporal rates of physiological and phenological processes in the ramets. NDVI values reflect orchard vigor during the evaluation period from a static point of view. Consequently, further research is needed to disentangle the responses of multispectral index values on temporal scales.

## 5. Conclusions

The major goal of this research was to extract tree-level attributes from a UAV. Estimates of total height, diameter, and crown surface were consistent with those reported in the literature. Furthermore, allometric relationships proved to be efficient in predicting diameter at breast height and basal diameter from attributes calculated with the UAV. The diversity of the used indices described the phytosanitary status of the orchard, with NDVI as the most recommended to evaluate productivity without discarding periodic evaluations. In this way, our hypothesis was confirmed; these measurements are reliable, and contribute to making solid and better-informed decisions on the individual-tree level. The application of the proposed workflow demonstrated solid parameters in estimates with consistent time saving and effort. Consistency in the measurement of tree-level characteristics on the individual-tree level has potential applications to improve current inventories. Nevertheless, recognizing its scopes and limitations, it is advisable to be cautious with the application of this approach in areas of greater complexity, such as the one studied here. Therefore, it is desirable to test different flight configurations and repeat missions to optimize the results and enrich the usefulness of the data.

**Author Contributions:** M.P.-G. planned and designed the research; J.L.G.-S. gathered field data; M.P.-G. and J.L.G.-S. contributed to data analysis; and M.P.-G. led the manuscript with contributions from J.L.G.-S. All authors have read and agreed to the published version of the manuscript.

**Funding:** This research and the APC was funded by CONACyT and COCYTED grant number A1-S-21471.

**Acknowledgments:** The authors are grateful to the Mexican National Science and Technology Council (CONACYT) for supporting the studies of the first author. We recognize CONACyT and COCYTED projects (A1-S-21471), as well <https://dendrored.ujed.mx/> and Ejido Papajichi for the facilities provided. Also, we acknowledge to the UTT students for helping to gather the field data.

**Conflicts of Interest:** The authors declare no conflict of interest.

## References

1. Brockerhoff, E.G.; Barbaro, L.; Castagneyrol, B.; Forrester, D.I.; Gardiner, B.; González-Olabarria, J.R.; Lyver, P.O.B.; Meurisse, N.; Oxbrough, A.; Taki, H.; et al. Forest biodiversity, ecosystem functioning and the provision of ecosystem services. *Biodivers. Conserv.* **2017**, *26*, 3005–3035. [[CrossRef](#)]
2. Holopainen, M.; Vastaranta, M.; Hyyppä, J. Outlook for the Next Generation's Precision Forestry in Finland. *Forests* **2014**, *5*, 1682–1694. [[CrossRef](#)]
3. Williams, A.P.; Allen, C.D.; Macalady, A.K.; Griffin, D.; Woodhouse, C.A.; Meko, D.M.; Swetnam, T.W.; Rauscher, S.A.; Seager, R.; Grissino-Mayer, H.D.; et al. Temperature as a potent driver of regional forest drought stress and tree mortality. *Nat. Clim. Chang.* **2013**, *3*, 292–297. [[CrossRef](#)]
4. Fornal-Pieniak, B.; Ollik, M.; Schwerk, A. Impact of different levels of anthropogenic pressure on the plant species composition in woodland sites. *Urban For. Urban Green.* **2019**, *38*, 295–304. [[CrossRef](#)]
5. Hedwall, P.-O.; Gustafsson, L.; Brunet, J.; Lindbladh, M.; Axelsson, A.-L.; Strengbom, J. Half a century of multiple anthropogenic stressors has altered northern forest understory plant communities. *Ecol. Appl.* **2019**, *29*, e01874. [[CrossRef](#)]
6. Gallardo-Salazar, J.L.; Pompa-García, M.; Aguirre-Salado, C.A.; López-Serrano, P.M.; Meléndez-Soto, A. Drones: Tecnología con futuro promisorio en la gestión forestal. *Rev. Mex. Cienc. For.* **2020**, *11*. [[CrossRef](#)]

7. Gollob, C.; Ritter, T.; Nothdurft, A. Forest Inventory with Long Range and High-Speed Personal Laser Scanning (PLS) and Simultaneous Localization and Mapping (SLAM) Technology. *Remote Sens.* **2020**, *12*, 1509. [[CrossRef](#)]
8. Lefsky, M.A.; Cohen, W.B.; Parker, G.G.; Harding, D.J. Lidar Remote Sensing for Ecosystem Studies. *BioScience* **2002**, *52*, 19–30. [[CrossRef](#)]
9. Puliti, S.; Breidenbach, J.; Astrup, R. Estimation of Forest Growing Stock Volume with UAV Laser Scanning Data: Can It Be Done without Field Data? *Remote Sens.* **2020**, *12*, 1245. [[CrossRef](#)]
10. Bokalo, M.; Stadt, K.J.; Comeau, P.G.; Titus, S.J. The Validation of the Mixedwood Growth Model (MGM) for Use in Forest Management Decision Making. *Forests* **2013**, *4*, 1–27. [[CrossRef](#)]
11. Li, Y.; Wang, W.; Zeng, W.; Wang, J.; Meng, J. Development of Crown Ratio and Height to Crown Base Models for Masson Pine in Southern China. *Forests* **2020**, *11*, 1216. [[CrossRef](#)]
12. Corona, P.; Chianucci, F.; Quatrini, V.; Civitarese, V.; Clementel, F.; Costa, C.; Floris, A.; Menesatti, P.; Puletti, N.; Sperandio, G.; et al. Precision forestry: Riferimenti concettuali, strumenti e prospettive di diffusione in Italia. *Forest@ Riv. Selvic. Ecol. For.* **2017**, *14*, 1–12. [[CrossRef](#)]
13. Modica, G.; Messina, G.; De Luca, G.; Fiozzo, V.; Praticò, S. Monitoring the vegetation vigor in heterogeneous citrus and olive orchards. A multiscale object-based approach to extract trees' crowns from UAV multispectral imagery. *Comput. Electron. Agric.* **2020**, *175*, 105500. [[CrossRef](#)]
14. Xue, J.; Su, B. Significant Remote Sensing Vegetation Indices: A Review of Developments and Applications. *J. Sens.* **2017**, *2017*, 1353691. [[CrossRef](#)]
15. Motohka, T.; Nasahara, K.N.; Oguma, H.; Tsuchida, S. Applicability of Green-Red Vegetation Index for Remote Sensing of Vegetation Phenology. *Remote Sens.* **2010**, *2*, 2369–2387. [[CrossRef](#)]
16. Bray, D.B.; Merino-Pérez, L.; Barry, D. *The Community Forests of Mexico: Managing for Sustainable Landscapes*; University of Texas Press: Austin, TX, USA, 2005.
17. Alvarado-Barrera, R.; Pompa-García, M.; Zúñiga-Vásquez, J.M.; Jiménez-Casas, M. Spatial analysis of phenotypic variables in a clonal orchard of *Pinus arizonica* Engelm. in northern Mexico. *Rev. Chapingo Ser. Cienc. For. Ambiente* **2019**, *25*, 185–199. [[CrossRef](#)]
18. Farjon, A. *A Handbook of the World's Conifers*; Brill: Leiden, The Netherlands, 2010; Volume 1, p. 1111.
19. Dempewolf, J.; Nagol, J.; Hein, S.; Thiel, C.; Zimmermann, R. Measurement of Within-Season Tree Height Growth in a Mixed Forest Stand Using UAV Imagery. *Forests* **2017**, *8*, 231. [[CrossRef](#)]
20. Mazzetto, F.; Calcante, A.; Mena, A.; Vercesi, A. Integration of optical and analogue sensors for monitoring canopy health and vigour in precision viticulture. *Precis. Agric.* **2010**, *11*, 636–649. [[CrossRef](#)]
21. Caruso, G.; Tozzini, L.; Rallo, G.; Primicerio, J.; Moriondo, M.; Palai, G.; Gucci, R. Estimating biophysical and geometrical parameters of grapevine canopies ('Sangiovese') by an unmanned aerial vehicle (UAV) and VIS-NIR cameras. *Vitis* **2017**, *56*, 63–70. [[CrossRef](#)]
22. Uribeetxebarria, A.; Daniele, E.; Escolà, A.; Arnó, J.; Martínez-Casasnovas, J.A. Spatial variability in orchards after land transformation: Consequences for precision agriculture practices. *Sci. Total Environ.* **2018**, *635*, 343–352. [[CrossRef](#)]
23. Arnó-Satorra, J.; Martínez-Casasnovas, J.A.; Ribes Dasi, M.; Rosell Polo, J.R. Review. Precision Viticulture. Research topics, challenges and opportunities in site-specific vineyard management. *Span. J. Agric. Res.* **2009**, *7*. [[CrossRef](#)]
24. Ballesteros, R.; Ortega, J.F.; Hernandez, D.; Moreno, M.A. Onion biomass monitoring using UAV-based RGB imaging. *Precis. Agric.* **2018**, *19*, 840–857. [[CrossRef](#)]
25. Tu, Y.-H.; Johansen, K.; Phinn, S.; Robson, A. Measuring Canopy Structure and Condition Using Multi-Spectral UAS Imagery in a Horticultural Environment. *Remote Sens.* **2019**, *11*, 269. [[CrossRef](#)]
26. Jorge, J.; Vallbé, M.; Soler, J.A. Detection of irrigation inhomogeneities in an olive grove using the NDRE vegetation index obtained from UAV images. *Eur. J. Remote Sens.* **2019**, *52*, 169–177. [[CrossRef](#)]
27. Jiménez-Brenes, F.M.; López-Granados, F.; de Castro, A.I.; Torres-Sánchez, J.; Serrano, N.; Peña, J.M. Quantifying pruning impacts on olive tree architecture and annual canopy growth by using UAV-based 3D modelling. *Plant Methods* **2017**, *13*, 55. [[CrossRef](#)] [[PubMed](#)]
28. Salamí, E.; Gallardo, A.; Skorobogatov, G.; Barrado, C. On-the-Fly Olive Tree Counting Using a UAS and Cloud Services. *Remote Sens.* **2019**, *11*, 316. [[CrossRef](#)]
29. Leduc, M.-B.; Knudby, A.J. Mapping Wild Leek through the Forest Canopy Using a UAV. *Remote Sens.* **2018**, *10*, 70. [[CrossRef](#)]

30. Jun, W.; Zhongkui, D.; Guoqing, Z. Geo-registration and mosaic of UAV video for quick-response to forest fire disaster. In Proceedings of the MIPPR 2007: Pattern Recognition and Computer Vision, Wuhan, China, 15 November 2007; Volume 678810.
31. Suziedelyte Visockiene, J.; Brucas, D.; Ragauskas, U. Comparison of UAV images processing softwares. *J. Meas. Eng.* **2014**, *2*, 111–121.
32. Mesas-Carrascosa, F.-J.; Notario García, M.D.; Meroño de Larriva, J.E.; García-Ferrer, A. An Analysis of the Influence of Flight Parameters in the Generation of Unmanned Aerial Vehicle (UAV) Orthomosaics to Survey Archaeological Areas. *Sensors* **2016**, *16*, 1838. [[CrossRef](#)]
33. Liba, N.; Berg-Jürgens, J. Accuracy of Orthomosaic Generated by Different Methods in Example of UAV Platform MUST Q. *IOP Conf. Ser. Mater. Sci. Eng.* **2015**, *96*, 012041. [[CrossRef](#)]
34. Agüera-Vega, F.; Carvajal-Ramírez, F.; Martínez-Carricondo, P. Accuracy of Digital Surface Models and Orthophotos Derived from Unmanned Aerial Vehicle Photogrammetry. *J. Surv. Eng.* **2017**, *143*, 04016025. [[CrossRef](#)]
35. Giannetti, F.; Puletti, N.; Puliti, S.; Travaglini, D.; Chirici, G. Assessment of UAV photogrammetric DTM-independent variables for modelling and mapping forest structural indices in mixed temperate forests. *Ecol. Indic.* **2020**, *117*, 106513. [[CrossRef](#)]
36. González-Elizondo, M.S.; González-Elizondo, M.; Tena-Flores, J.A.; Ruacho-González, L.; López-Enríquez, I.L. Vegetación de la Sierra Madre Occidental, México: Una síntesis. *Acta Bot. Mex.* **2012**, *100*, 351–403. [[CrossRef](#)]
37. González-Cásares, M.; Pompa-García, M.; Camarero, J.J. Differences in climate–growth relationship indicate diverse drought tolerances among five pine species coexisting in Northwestern Mexico. *Trees* **2017**, *31*, 531–544. [[CrossRef](#)]
38. P4 Multispectral. Available online: [www.dji.com/mx/p4-multispectral](http://www.dji.com/mx/p4-multispectral) (accessed on 3 September 2020).
39. Lu, H.; Fan, T.; Ghimire, P.; Deng, L. Experimental Evaluation and Consistency Comparison of UAV Multispectral Minisensors. *Remote Sens.* **2020**, *12*, 2542. [[CrossRef](#)]
40. DJI Ground Station Pro. Available online: [www.dji.com/mx/ground-station-pro](http://www.dji.com/mx/ground-station-pro) (accessed on 3 September 2020).
41. Syetiawan, A.; Gularso, H.; Kusnadi, G.I.; Pramudita, G.N. Precise topographic mapping using direct georeferencing in UAV. *IOP Conf. Ser. Earth Environ. Sci.* **2020**, *500*, 012029. [[CrossRef](#)]
42. P4 Multispectral Specs. Available online: <https://www.dji.com/p4-multispectral/specs> (accessed on 23 November 2020).
43. OpenDroneMap. Available online: [www.opendronemap.org](http://www.opendronemap.org) (accessed on 10 September 2020).
44. Groos, A.R.; Bertschinger, T.J.; Kummer, C.M.; Erlwein, S.; Munz, L.; Philipp, A. The Potential of Low-Cost UAVs and Open-Source Photogrammetry Software for High-Resolution Monitoring of Alpine Glaciers: A Case Study from the Kanderfirn (Swiss Alps). *Geosciences* **2019**, *9*, 356. [[CrossRef](#)]
45. Burdziakowski, P. Evaluation of Open Drone Map Toolkit for Geodetic Grade Aerial Drone Mapping—Case Study. *Int. Multidiscip. Sci. Geoconf.* **2017**, *17*, 101–109. [[CrossRef](#)]
46. Lee, S.; Yu, B.-H. Automatic detection of dead tree from UAV imagery. In Proceedings of the 39th Asian Conference on Remote Sensing, Kuala Lumpur, Malaysia, 15–19 October 2018.
47. QGIS. A Free and Open Source Geographic Information System. Available online: [www.qgis.org](http://www.qgis.org) (accessed on 10 September 2020).
48. Iizuka, K.; Yonehara, T.; Itoh, M.; Kosugi, Y. Estimating Tree Height and Diameter at Breast Height (DBH) from Digital Surface Models and Orthophotos Obtained with an Unmanned Aerial System for a Japanese Cypress (*Chamaecyparis obtusa*) Forest. *Remote Sens.* **2018**, *10*, 13. [[CrossRef](#)]
49. Ke, Y.; Quackenbush, L.J. A review of methods for automatic individual tree-crown detection and delineation from passive remote sensing. *Int. J. Remote Sens.* **2011**, *32*, 4725–4747. [[CrossRef](#)]
50. Larsen, M.; Eriksson, M.; Descombes, X.; Perrin, G.; Brandtberg, T.; Gougeon, F.A. Comparison of six individual tree crown detection algorithms evaluated under varying forest conditions. *Int. J. Remote Sens.* **2011**, *32*, 5827–5852. [[CrossRef](#)]
51. ForestTools: Analyzing Remotely Sensed Forest Data. Available online: <https://CRAN.R-project.org/package=ForestTools> (accessed on 15 September 2020).
52. The R Project for Statistical Computing. Available online: [www.r-project.org/](http://www.r-project.org/) (accessed on 15 September 2020).
53. Abdalla, A.; Elmahal, A. Augmentation of vertical accuracy of digital elevation models using Gaussian linear convolution filter. In Proceedings of the 2016 Conference of Basic Sciences and Engineering Studies SGCAC, Khartoum, Sudan, 20–23 February 2016; pp. 206–210.

54. The Whitebox Geospatial Analysis Tools Project and Open-Access GIS. Available online: <https://jblindsay.github.io/ghrg/WhiteboxTools/index.html> (accessed on 9 November 2020).
55. Popescu, S.C.; Wynne, R.H. Seeing the Trees in the Forest: Using Lidar and Multispectral Data Fusion with Local Filtering and Variable Window Size for Estimating Tree Height. *Photogramm. Eng. Remote Sens.* **2004**, *70*, 589–604. [[CrossRef](#)]
56. Beucher, S.; Meyer, F. The Morphological Approach to Segmentation: The Watershed Transformation. In *Mathematical Morphology in Image Processing*; Dougherty, E.R., Ed.; CRC Press: Boca Raton, FL, USA, 1993; Volume 34, pp. 433–481.
57. Gujarati, D.N. *Basic Econometrics*; The McGraw-Hill Education: New York, NY, USA, 2004.
58. Wang, Y.; Lehtomäki, M.; Liang, X.; Pyörälä, J.; Kukko, A.; Jaakkola, A.; Liu, J.; Feng, Z.; Chen, R.; Hyypä, J. Is field-measured tree height as reliable as believed—A comparison study of tree height estimates from field measurement, airborne laser scanning and terrestrial laser scanning in a boreal forest. *ISPRS J. Photogramm. Remote Sens.* **2019**, *147*, 132–145. [[CrossRef](#)]
59. DJI TERRA Index Descriptions. Available online: <https://www.dji.com/dji-terra> (accessed on 25 November 2020).
60. He, J.; Li, Y.; Zhang, K. Research of UAV Flight Planning Parameters. *Positioning* **2012**, *3*, 43–45. [[CrossRef](#)]
61. Gougeon, F.; Leckie, D. The Individual Tree Crown Approach Applied to Ikonos Images of a Coniferous Plantation Area. *Photogramm. Eng. Remote Sens.* **2006**, *72*, 1287–1297. [[CrossRef](#)]
62. Iglhaut, J.; Cabo, C.; Puliti, S.; Piermattei, L.; O'Connor, J.; Rosette, J. Structure from Motion Photogrammetry in Forestry: A Review. *Curr. For. Rep.* **2019**, *5*, 155–168. [[CrossRef](#)]
63. Krause, S.; Sanders, T.G.M.; Mund, J.-P.; Greve, K. UAV-Based Photogrammetric Tree Height Measurement for Intensive Forest Monitoring. *Remote Sens.* **2019**, *11*, 758. [[CrossRef](#)]
64. SEMARNAT-NOM-152. Available online: [http://www.diariooficial.gob.mx/nota\\_detalle.php?codigo=5064731&fecha=17/10/2008](http://www.diariooficial.gob.mx/nota_detalle.php?codigo=5064731&fecha=17/10/2008) (accessed on 20 September 2020).
65. Wu, D.; Johansen, K.; Phinn, S.; Robson, A.; Tu, Y.-H. Inter-comparison of remote sensing platforms for height estimation of mango and avocado tree crowns. *Int. J. Appl. Earth Obs. Geoinf.* **2020**, *89*, 102091. [[CrossRef](#)]
66. Roşca, S.; Suomalainen, J.; Bartholomeus, H.; Herold, M. Comparing terrestrial laser scanning and unmanned aerial vehicle structure from motion to assess top of canopy structure in tropical forests. *Interface Focus* **2018**, *8*, 20170038. [[CrossRef](#)]
67. Falkowski, M.J.; Smith, A.M.S.; Hudak, A.T.; Gessler, P.E.; Vierling, L.A.; Crookston, N.L. Automated estimation of individual conifer tree height and crown diameter via two-dimensional spatial wavelet analysis of lidar data. *Can. J. Remote Sens.* **2006**, *32*, 153–161. [[CrossRef](#)]
68. Johansen, K.; Raharjo, T.; McCabe, M.F. Using Multi-Spectral UAV Imagery to Extract Tree Crop Structural Properties and Assess Pruning Effects. *Remote Sens.* **2018**, *10*, 854. [[CrossRef](#)]
69. Ritter, T.; Nothdurft, A. Automatic Assessment of Crown Projection Area on Single Trees and Stand-Level, Based on Three-Dimensional Point Clouds Derived from Terrestrial Laser-Scanning. *Forests* **2018**, *9*, 237. [[CrossRef](#)]
70. Grulke, N.; Bienz, C.; Hrinkevich, K.; Maxfield, J.; Uyeda, K. Quantitative and qualitative approaches to assess tree vigor and stand health in dry pine forests. *For. Ecol. Manag.* **2020**, *465*, 118085. [[CrossRef](#)]
71. Zhao, H.; Yang, C.; Guo, W.; Zhang, L.; Zhang, D. Automatic Estimation of Crop Disease Severity Levels Based on Vegetation Index Normalization. *Remote Sens.* **2020**, *12*, 1930. [[CrossRef](#)]
72. Brovkina, O.; Cienciala, E.; Surový, P.; Janata, P. Unmanned aerial vehicles (UAV) for assessment of qualitative classification of Norway spruce in temperate forest stands. *Geo-Spatial Inf. Sci.* **2018**, *21*, 12–20. [[CrossRef](#)]
73. Wahab, I.; Hall, O.; Jirstrom, M. Remote Sensing of Yields: Application of UAV Imagery-Derived NDVI for Estimating Maize Vigor and Yields in Complex Farming Systems in Sub-Saharan Africa. *Drones* **2018**, *2*, 28. [[CrossRef](#)]
74. Bausch, W.C.; Halvorson, A.D.; Cipra, J. Quickbird satellite and ground-based multispectral data correlations with agronomic parameters of irrigated maize grown in small plots. *Biosyst. Eng.* **2008**, *101*, 306–315. [[CrossRef](#)]
75. Ren, H.; Zhou, G. Determination of green aboveground biomass in desert steppe using litter-soil-adjusted vegetation index. *Eur. J. Remote Sens.* **2014**, *47*, 611–625. [[CrossRef](#)]
76. Minařík, R.; Langhammer, J. Use of a multispectral UAV photogrammetry for detection and tracking of forest disturbance dynamics. *Int. Arch. Photogramm. Remote Sens. Spatial Inf. Sci.* **2016**, *XLI-B8*, 711–718. [[CrossRef](#)]
77. Xing, N.; Huang, W.; Xie, Q.; Shi, Y.; Ye, H.; Dong, Y.; Wu, M.; Sun, G.; Jiao, Q. A Transformed Triangular Vegetation Index for Estimating Winter Wheat Leaf Area Index. *Remote Sens.* **2020**, *12*, 16. [[CrossRef](#)]

78. Garrity, S.R.; Vierling, L.A.; Smith, A.M.S.; Falkowski, M.J.; Hann, D.B. Automatic detection of shrub location, crown area, and cover using spatial wavelet analysis and aerial photography. *Can. J. Remote Sens.* **2014**, *34*, S376–S384. [[CrossRef](#)]
79. Jing, L.; Hu, B.; Noland, T.; Li, J. An individual tree crown delineation method based on multi-scale segmentation of imagery. *ISPRS J. Photogramm. Remote Sens.* **2012**, *70*, 88–98. [[CrossRef](#)]

**Publisher’s Note:** MDPI stays neutral with regard to jurisdictional claims in published maps and institutional affiliations.



© 2020 by the authors. Licensee MDPI, Basel, Switzerland. This article is an open access article distributed under the terms and conditions of the Creative Commons Attribution (CC BY) license (<http://creativecommons.org/licenses/by/4.0/>).